Nature of electrical contacts in a metal–molecule–semiconductor system

J. W. P. Hsu,[a] Y. L. Loo,[b] D. V. Lang, and J. A. Rogers
Bell Laboratories, Lucent Technologies, Murray Hill, New Jersey 07974

(Received 19 January 2003; accepted 1 March 2003; published 5 August 2003)

The effects of the top electrode fabrication method on the transport properties of Au–alkanedithiol–GaAs junctions are examined. We found that diodes made by evaporating Au on 1,8-octanedithiol monolayer behave similarly to Au–GaAs junctions without the molecular layer. The direct Au–GaAs contact dominates the electrical conduction in these evaporated devices despite the presence of the molecular layer. In contrast, Au–dithiol–GaAs diodes made by nanotransfer printing (nTP) exhibit no direct contact between Au and GaAs. Electrical transport in the nTP junctions occurs through the 1,8-octanedithiol insulating layer. The low current levels and the high barrier-height values in the current–voltage results and the exponential energy dependence in the photoreponse yield that are observed in the nTP diodes support this conclusion. Since transport through the molecular layer is much less conductive, even a miniscule region of direct contact between the two electrodes will make it impossible to observe electrical transport through molecules. Fractional amounts of the different types of contacts for each kind of sample were obtained from the experimental results. © *2003 American Vacuum Society.* [DOI: 10.1116/1.1588641]

I. INTRODUCTION

As the field of molecular electronics advances, it is recognized that a better understanding of the properties of electrical contacts between electrodes and molecules is needed. Since electrical measurements on molecular systems are two point rather than four point, the electrical properties of the contacts are experimentally difficult to separate from those of the molecules. To approach this problem, most researchers vary the molecules while using the same electrodes.[1] While this is a valid idea, the electrical properties of a metal–molecule bond are sensitive to perturbation, e.g., Au–S bond length, and hence can be different for different molecules. Another approach is to vary the metals used as electrodes. Recently, the contact resistance to alkanedithiols was found to depend on the metal work function.[2] In this experiment, we kept the materials used for electrodes (Au and GaAs) and the molecule (1,8-octanedithiols) constant. Instead, the *method* of fabricating the top Au electrode was varied. For a different molecule and using lift-off float-on metal contacts,[3] Vilan and Cahen found qualitative differences in the electrical properties of contacts depending on the details of a single fabrication procedure. Here we quantitatively compare the characteristics of electrical contacts that are made by different physical methods. We find that the electrical properties of the two-terminal devices depend strongly on *how* the contacts are fabricated and present quantitative results on the different types of contacts for each kind of devices.

Evaporation is the most commonly used method to deposit metal electrodes on molecules. Since the chemicals and ultraviolet light used in conventional lithography could damage the molecular layers, most metal electrodes on top of molecular layers are deposited through shadow masks, and hence are typically large in size ($>10\ \mu$m). Devices with contacts made by evaporation have a very low yield due to shorting between the two electrodes.[4] X-ray photoelectron spectroscopy (XPS) studies showed that in some systems the evaporated metal penetrates the molecular layer and contacts the substrate metal, i.e., the bottom electrode in molecular diodes.[5] In addition, damages to the molecular layer by incoming high-energy atoms can occur.[6] Recently, it is demonstrated that nanotransfer printing (nTP) is a superior method for fabricating metal electrodes in plastic electronics[7] and molecular diodes.[8] In nTP, chemical bonds are formed between the substrate surface and the transferred metal patterns. This process takes place *under ambient conditions*. In this article, we compare the electrical properties of Au–dithiol–GaAs devices with top Au electrodes made using nTP to those made by evaporation to elucidate the role of fabrication methods on device performance.

Instead of metal substrates that are commonly used in molecular electronic studies, we chose GaAs for several reasons. GaAs surfaces are smooth and do not contain defects such as grain boundaries, which might affect monolayer formation. Self-assembled monolayers of thiol[9,10] and dithiol[11] molecules on GaAs have been reported. Most importantly, using a semiconductor as one of the electrodes enables us to evaluate the nature of the contacts quantitatively based on well-established models for electrical transport between metals and semiconductors. Au forms a Schottky contact with low-carrier-density n-type GaAs with a barrier height of 0.9 V.[12,13] This value is lowered to ~ 0.7 V due to the image force for the degenerately doped n^+ GaAs (1.5×10^{18} cm^{-3}) used in this experiment.[14] These highly doped GaAs wafers were chosen to minimize series resistance in the bottom electrode. The presence of the molecular layer between Au and GaAs will lead to changes in the Au–GaAs Schottky contact properties. If we were to use Au for both

[a]Author to whom correspondence should be addressed; electronic mail: jhsu@mailaps.org
[b]Current address: Dept. of Chemical Engineering, University of Texas at Austin, Austin, TX 78712.

electrodes, only current–voltage ($I-V$) information can be obtained. In this experiment, photoresponse and capacitance–voltage ($C-V$) experiments were performed on Au–dithiol–GaAs junctions in addition to the $I-V$ measurements to gain a better picture of the nature of electrical contacts.

II. EXPERIMENT

A. Nanotransfer printing

In nTP, metal patterns are transferred from an elastomeric stamp onto a molecular layer chemically bonded to a substrate. The interfacial chemistry was tailored to facilitate the printing process for a given molecular end group and the surface of the transferred metal patterns. In this experiment, the native oxide on the GaAs wafers was first stripped by immersing them in a concentrated NH_4OH or HCl solution for 2 min. We do not observe any difference in the nTP results between the acid and base treatments. Immediately after oxide removal, the 1,8-octanedithiol (used as received from Aldrich Chemical Co.) layer is formed by placing the freshly etched wafers in a vacuum chamber along with several drops of 1,8-octanedithiol placed on a heated aluminum block. After deposition, the wafers are rinsed thoroughly with ethanol to remove possible multilayers. Immersing the freshly etched wafers in a dilute ethanolic solution of 1,8-octanedithiol also produces comparable results. Based on surface treatment experiments,[15] the majority of the molecules chemisorb on the surface with one thiol endgroup and have unreacted thiol endgroups away from the GaAs surface.

The elastomeric stamps used in nTP are fabricated by casting and curing polydimethylsiloxane (PDMS) prepolymer (Sylgard 184 from Dow Chemical Co.; A:B=1:10) against silicon wafers whose relief features are predefined by photoresist. A thin film of Au is then evaporated onto the stamp. The adhesion of Au to PDMS is inherently poor. When the freshly Au–coated PDMS stamp is brought into contact with the dithiol-treated substrate, the free thiol endgroups on the GaAs substrate reacts spontaneously with Au in the regions of contact. This reaction produces permanent Au–S bonds. The elasticity and the mechanical comformability of the PDMS stamp ensure good contact at the stamp/substrate interface without the need to apply pressure. Removing the stamp from the substrate completes the pattern transfer process. The monolayer behaves like an adhesion layer; it chemically bonds the Au pattern to the substrate. Details of the nTP procedures and characterization of these structures are published elsewhere.[7,15]

B. Characterization of free thiol endgroups

Fourier transform infrared (FTIR) spectra were taken in transmission on a sample with the dithiol layer deposited as described in the previous section. The spectra show distinct polarization dependence with the CH_2 stretching modes measured at 2854 cm^{-1} (symmetric) and 2927 cm^{-1} (asymmetric), which are similar but higher than the frequencies of the same modes measured on longer-chain alkanethiol on GaAs.[9,10] This is consistent with the expectation that long-chain molecules form a more ordered monolayer than short-chain molecules and monothiols are more ordered than dithiols. Thus, the majority of the octanedithiol molecules are probably not lying flat on the GaAs surface. To further confirm the presence of free thiol end groups, in addition to the surface treatment studies, freshly etched and dithiol treated GaAs wafers were soaked in a 5 nm gold sol aqueous solution[16] and rinsed thoroughly with de-ionized water. Atomic force microscopy (AFM) images show a full coverage[17] ($>3\times10^{11}$ cm^{-2}) of 5 nm gold particles on the dithiol treated surface, compared to $<1\times10^{10}$ cm^{-2} on the etched GaAs surface without a dithiol layer. AFM imaging after Scotch tape adhesion tests showed that gold nanoparticles remain on the dithiol-treated surface with the same (full) coverage. We also made molecular diodes by transferring Au patterns from PDMS stamps to such Au–colloid–coated, dithiol-treated GaAs surfaces via a cold welding mechanism.[18] Junctions on this Au–Au colloids–dithiol–GaAs sample also pass the scotch tape test and have transport characteristics similar to regular nTP Au–dithiol–GaAs junctions. Based on the combination of the FTIR results and the fact that the transferred Au patterns and Au colloids deposited on the dithiol-treated GaAs wafers pass the Scotch tape test, we conclude that the dithiol molecules form a monolayer on the GaAs surface with the majority having a free thiol endgroup to bond with Au. However, there is probably little long-range in-plane order.

C. Reference samples

To evaluate the effects of the electrode fabrication method on the properties of electrical contacts, we compare nTP junctions to evaporated junctions (*evaporated* and *cold-evaporated*), in which the Au top electrodes were deposited directly on the dithiol layer by electron beam evaporation. The dithiol layer formation in these evaporated junctions was done in an identical way as described above for the nTP junctions. To distinguish electrical transport through the molecules from that due to direct Au–GaAs contacts, we also made control samples (*control* and *cold-control*) where Au is directly evaporated on the GaAs surface, i.e., no dithiol molecules. Furthermore, some samples were cooled to $-15\,^{\circ}C$ during Au evaporation (*cold-control* and *cold-evaporated*) to evaluate the common belief that cooling samples reduces shorting between electrodes.[4] The thickness of the Au pads on all samples is $\sim$20 nm, deposited at 1 nm/sec. Sample names and the method and condition used to fabricate the top Au electrodes are listed in Table I.

III. RESULTS

A. *I–V*

Figure 1(a) shows the absolute values of current density (J) versus bias voltage applied to the top Au electrode (V) for all five types of samples. The $J-V$ curves are linear for reverse (negative) bias and superlinear for forward (positive) bias; this behavior is more clearly shown in Fig. 1(b) where

TABLE I. Sample name, structure, specific resistance obtained from linear regions of the $I-V$ curves (R) and junction area (A), zero-bias barrier height obtained from $I-V$ ($\Phi_{IV}(0)$), ideality factor (n) obtained from fitting forward-bias $I-V$ curves, slope of barrier vs bias ($d\Phi_{IV}/dV$), barrier height obtained from IPE data ($\Phi_{\mathrm{IPE}}(0)$), characteristic energy (E_0) in the exponential energy dependence of photoresponse yield, and barrier height obtained from reverse-bias $C-V$ (Φ_{CV}).

Sample name	Structure and fabrication methods	RA[a] (Ω cm^2)	$\Phi_{IV}(0)$ (V)	n	$\frac{d\Phi_{IV}}{dV}$	$\Phi_{\mathrm{IPE}}(0)$ (V)	E_0 (meV)	Φ_{CV}[a] (V)
control	Au–GaAs	43.1 ± 5.2	0.54	1.62	0.38	0.76	[b]	1.02 ± 0.02
cold-control	Au–GaAs $-15\,^{\circ}$C	79.7 ± 8.6	0.55	1.59	0.38	0.68	[b]	1.01 ± 0.01
evaporated	Au–dithiol–GaAs	141 ± 15	0.58	1.66	0.37	0.68	[b]	NA[d]
cold-evaporated	Au–dithiol–GaAs, $-15\,^{\circ}$C	1166 ± 544	0.63	1.70	0.41	0.68[c]	50[c]	NA[d]
nTP	Au–dithiol–GaAs	$(1.22\pm0.24)\times10^7$	0.87	1.42	0.32	[b]	50	2.35 ± 0.12

[a]Error values represent 1 s.d. of the diodes measured.
[b]The value cannot be obtained from the data because the data have a different dependence.
[c]Different energy dependence for different energy range.
[d]Not available.

normalized J versus V curves are displayed in linear scale. These $J-V$ behaviors are far from ideal Schottky junctions and can be modeled by a circuit of a diode in parallel with a shunt resistor (or very low-barrier-height contacts). The specific resistance (RA, where A is the junction geometric area) obtained from the slope of reverse bias $J-V$ curves is an indication of the fraction of conduction through low-barrier channels. Astoundingly, the RAs for the Au–dithiol–GaAs devices made by nTP (Sample *nTP*)[19] are 4–5 orders of magnitude larger than RAs for diodes with evaporated Au contacts (*evaporated* and *cold-evaporated*) (Table I).

For Schottky contacts, the ideality factor (n) is used to characterize the deviation of measured $J-V$ behavior from ideal Schottky contact characteristics. One obtains n from fitting the measured forward-bias $J-V$ curve to a phenomenological thermionic model[20]

$$J(V)=A^*T^2\exp\left(-\frac{q\Phi_{IV}}{kT}\right)\cdot\left[\exp\frac{qV}{nkT}-1\right], \tag{1}$$

where k is the Boltzmann constant, T is temperature, q is the fundamental charge, A^* is the effective Richardson constant ($=8.6$ A/cm^2 K^2 for n–GaAs),[21] and Φ_{IV} is the Schottky barrier height which is assumed to be voltage independent. We note that $n=1$ for ideal and $n>1$ for nonideal Schottky contacts. Fitting $J-V$ data of our devices to Eq. (1) produces n between 1.4 and 1.7 (Table I), highly nonideal. The nonideality arises from the bias dependence of the barrier height[20]

$$n=\left(1-\frac{d\Phi_{IV}}{dV}\right)^{-1}. \tag{2}$$

Another way to examine the $J-V$ characteristics is to evaluate the barrier height at each bias using[22,23]

$$\Phi_{IV}(V)=\frac{kT}{q}\left[\ln(A^*T^2)-\ln\frac{J}{\left(\exp\frac{qV}{kT}\right)-1}\right]. \tag{3}$$

Figure 1(c) is a plot of Φ_{IV} (V) versus V for all samples. It is clear that Φ_{IV} varies linearly with V with $d\Phi_{IV}/dV$ ranging from 0.32 to 0.41 (Table I). The values of n obtained from the measured $d\Phi_{IV}/dV$ using Eq. (2) agree with those obtained from fitting $J-V$ curves to Eq. (1), indicative of the robustness of the analysis. Note that Eq. (1) applies to forward bias while Eq. (3) can be used for both forward and reverse bias.[22] The difference between the *nTP* and evaporated junctions is clearly reflected in the barrier height (Table I). Since J depends exponentially on Φ_{IV} [Eq. (1)], the higher Φ_{IV} is responsible for the overall lower J observed for the *nTP* sample.

B. Internal photoemission

Measuring photoresponse yield (Y), photocurrent per absorbed photon, as a function of photon energy (E) is a well established, but less used, method for determining Schottky barrier heights.[24] Figure 2(a) shows Y (log scale) versus E taken under no bias for all samples. For photon energies below the GaAs band gap (1.4 eV), the dominant mechanism producing photocurrent is for an electron in the Au electrode to absorb the photon energy and overcome the Schottky barrier. This is analogous to an emission of an electron from metals into vacuum and hence the name internal photoemission (IPE). Y is proportional to $(E-\Phi_{\mathrm{IPE}})^2$ for metal–semiconductor Schottky diodes.[25] The subscript "IPE" is used to differentiate it from the barrier height determined from $I-V$. Figure 2(b) shows $\sqrt{Y}$ versus E near Φ_{IPE} for the *cold-control*, *evaporated*, and *nTP* samples. It is clear that the *cold-control* and *evaporated* samples display this classic energy dependence (solid lines) of Schottky contacts with $\Phi_{\mathrm{IPE}}\sim0.7$ V, consistent with the expected barrier height for Au on 10^{18} cm^{-3} n^+ GaAs including image force lowering.[12,14] However, the *nTP* sample cannot be described by this energy dependence. Attempts to extract a barrier height from this data using $(E-\Phi_{\mathrm{IPE}})^2$ produce $\Phi_{\mathrm{IPE}}>1$ V, a value that is unreasonable for the Au–GaAs

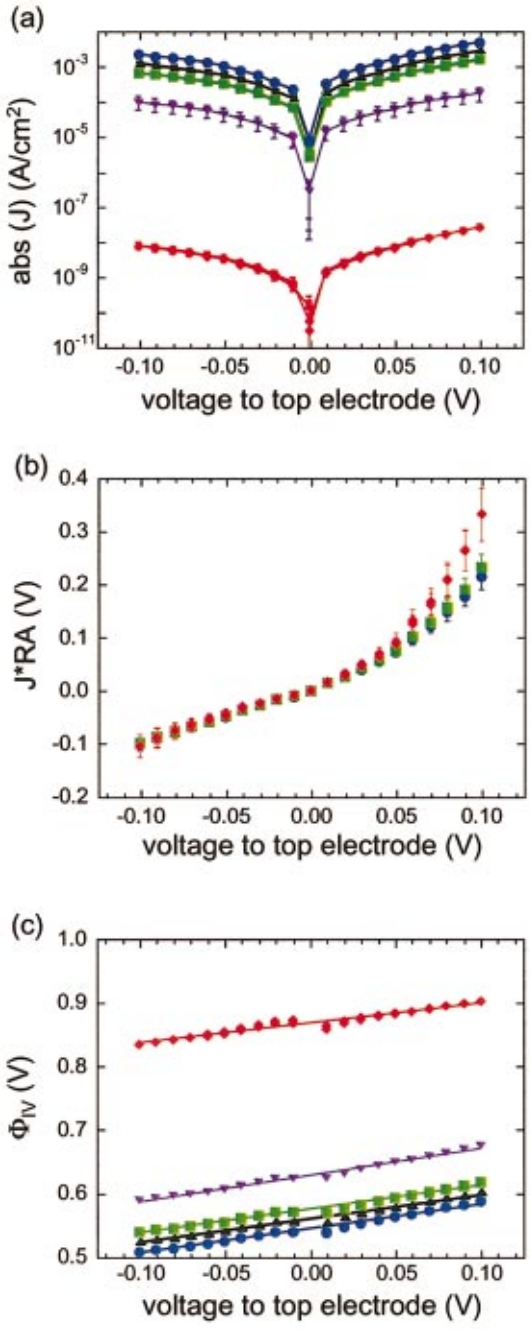

FIG. 1. Current–voltage characteristics of two-terminal Au–GaAs and Au–dithiol–GaAs junctions with the Au electrodes made by different methods. (a) Absolute values of current density (J) (log scale) vs bias to top Au electrode (V). (b) Normalized J vs V in linear scale for the control, evaporated, and nTP samples. Normalized J is obtained by multiplying J by RA (Table I). We have to normalize J to display these curves on the same scale due to the wide range of the current levels. (c) Schottky barrier height (Φ_{IV}) vs V, with Φ_{IV} obtained from data shown in (a) using Eq. (3). *Control*: blue circles; *cold-control*: black triangles; *evaporated*: green squares; *cold-evaporated*: purple upside-down triangles; *nTP*: red diamonds. The data were averaged over 17 diodes for the *nTP* sample and ten diodes for the other four samples. In (a), standard deviations are shown as error bars and visible for *cold-evaporated* and *nTP*; the size of the symbols is larger than error bars for the rest of the samples.

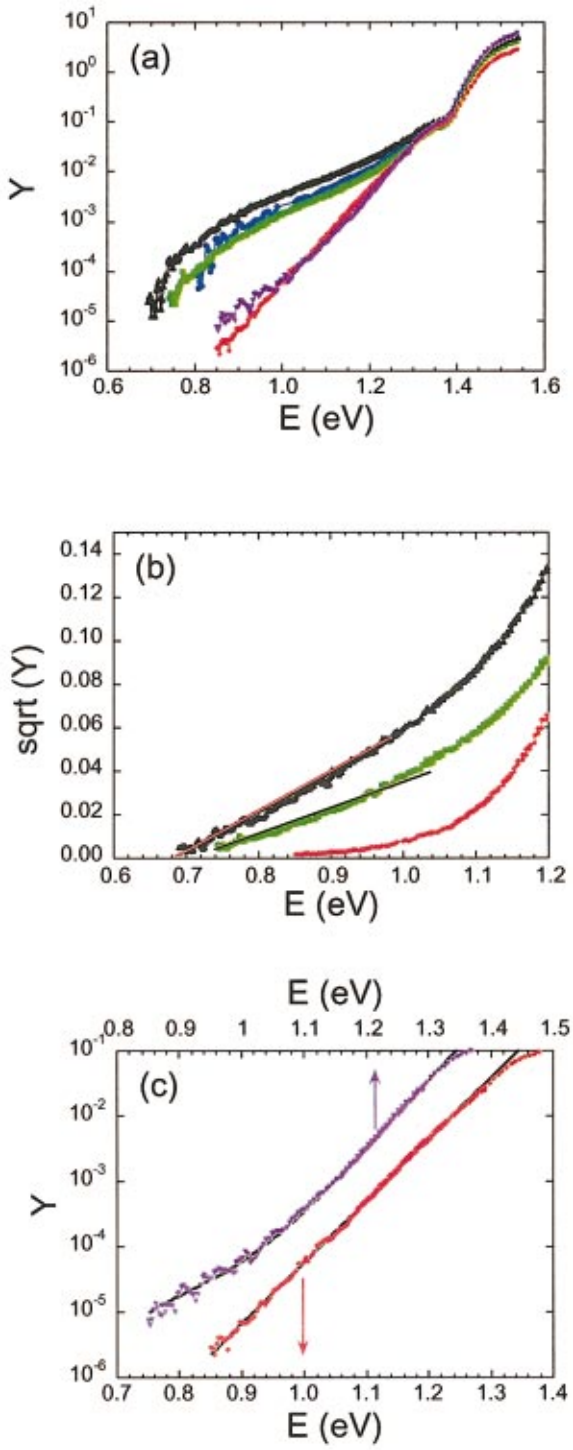

FIG. 2. Photoresponse yield (Y) vs photon energy (E) for all samples (Table I). (a) Y (log scale) vs E for all samples. (b) $\sqrt{Y}$ vs E for $E<1.2$ eV for the *cold-control, evaporated,* and *nTP* samples. (c) Y (log scale) vs E for $E<1.4$ eV for the *cold-evaporated* and *nTP* samples. *Control*: blue circles; *cold-control*: black triangles; *evaporated*: green squares; *cold-evaporated*: purple upside-down triangles; *nTP*: red diamonds. The solid lines in (b) represent $\sqrt{Y} \propto (E-\Phi_{\mathrm{IPE}})$. In (c), The *cold-evaporated* sample uses the upper x axis and is offset from the lower x axis (for the *nTP* sample) by 0.1 eV for clarity. The lines are fit to the data.

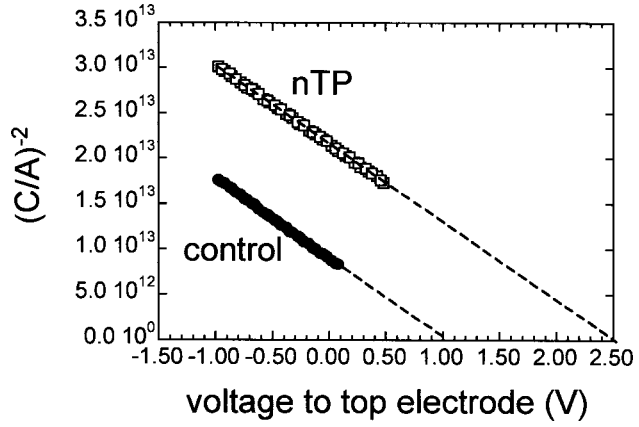

FIG. 3. Square of the inverse depletion-layer capacitance per unit area $((C/A)^{-2})$ vs bias voltage applied to the top Au electrode (V) for *control* (solid circles) and *nTP* (open squares) samples. The dashed lines are extrapolated linear fits to the data. The slope is inversely proportional to the dopant density and the intercept with the voltage axis is the barrier height.

Schottky barrier height. Instead, the *nTP* sample shows an exponential E dependence over 3 1/2 decades in the IPE yield [Fig. 2(c)]. This exponential E dependence is not characteristic of metal–semiconductor Schottky contacts; rather, it indicates the presence of disordered material in the emitter. Interestingly, the *cold-evaporated* sample, for which the Au evaporation was done at $-15\,^{\circ}\mathrm{C}$, also displays this exponential dependence but with a tail at low energy. The solid line is a model that combines the exponential dependence and $(E-\Phi_{\mathrm{IPE}})^2$. The energy dependence of the IPE yield of the *cold-evaporated* and *nTP* samples will be discussed later in the article.

C. *C–V*

For Schottky diodes, the barrier height can also be obtained from the voltage dependence of depletion-layer capacitance C, by determining the intercept with the voltage axis of the linear $1/C^2$ versus V curve.[26] Note that Φ_{CV} does not include the image force lowering effect and should be higher than Φ_{IV} and Φ_{IPE}. Figure 3 shows $C-V$ results for the *control* and *nTP* samples. Reverse bias $C-V$ measurements on control samples (*control* and *cold-control*) produce a barrier height Φ_{CV} of ~ 1.0 V, consistent with reported $C-V$ barrier height for Au–GaAs.[27] Reverse-bias $C-V$ behavior in the *nTP* sample is similar to that of *control* samples, i.e., $1/C^2$ is linearly proportional to V. However, the Φ_{CV} obtained by extrapolating to zero $1/C^2$ is 2.35 V, significantly higher than Φ_{CV} for Au–GaAs. The difference between 2.35 and 1.0 V is ~ 20 times too large to be accounted for by extrapolating the band bending in the GaAs through a 1-nm-thick insulating layer.[28] Hence, we attribute the difference in the intercept voltage to a flatband voltage shift. The measured sign corresponds to negative charges trapped in the dithiol layer near the GaAs surface and positive charges in the Au.[29] The formation of interfacial dipoles has been reported for several organic–inorganic interfaces and has an effect on band alignment and transport properties.[30] One source of interfacial dipole in our system comes from the charge transfer that occurs when S bonds to Au or GaAs. Dipoles in the dithiol layer would result if the amount of charge transferred were different for S–Au compared to S–GaAs bonds. The $C-V$ results imply that more negative charges are transferred to the molecular from GaAs than from Au. Assuming 1 nm length and a density of 10^{14} cm^{-2} for the molecular layer, a 1 V shift in Φ_{CV} corresponds to 0.1 e, which is a reasonable value for the charge imbalance between S–Au and S–GaAs bonds.[31]

IV. DISCUSSION

A. Control junctions: Au–GaAs Schottky diodes

It is important to have some understanding of the Au–GaAs Schottky diodes (*control* and *cold-control* samples) before trying to analyze the Au–dithiol–GaAs structures. The nonideal Schottky behavior we observed in the *control* diodes arises from the high doping density of the n-GaAs as well as the high degree of reactivity between Au and GaAs. For GaAs of 1.5×10^{18} cm^{-3} electron density, the electrical transport between the metal and GaAs at room temperature is dominated by thermionic field emission (TFE).[32] However, TFE alone cannot explain the large values of n that we measured in these devices. In fact, none of the standard mechanisms, such as image force lowering of barrier heights, interfacial layers, or recombination in the depletion region, is consistent with the data. However, all of these models assume that the Schottky contact is spatially homogeneous. Recently, nonideality arising from barrier-height inhomogeneity has been investigated.[33,34] It was found that inhomogeneous Schottky junctions show voltage dependent barrier heights and hence nonideal behavior.

Ballistic electron emission microscopy images show that the Au–GaAs Schottky barrier is highly nonuniform,[35] consistent with the high reactivity between Au and GaAs.[36] The transport results we observed in the *control* and *cold-control* samples are consistent with the existence of inhomogeneous Schottky barrier heights in Au–GaAs diodes. The fact that Φ_{IV} (0.55 V) is lower than Φ_{IPE} (0.7 V) is one clear indication of barrier-height inhomogeneity. Assuming there is a distribution of barrier heights, current under bias depends on the barrier height exponentially [Eq. (1)] and is dominated by the lower-barrier-height regions. Photocurrent, on the other hand, sums the different contributions according to their effective areas and will be much less sensitive to small regions of lower-barrier-height contact. The experimental value of $\Phi_{CV}\sim 1.0$ eV is also consistent with the inhomogeneous model since $C-V$ measures the mean barrier height and is not sensitive to the presence of low-barrier-height regions.[34] By comparing the RA from the $I-V$ results to the specific contact resistance of a good ohmic contact on n^+ GaAs ($10^{-6}\ \Omega\,\mathrm{cm}^2$),[37] the fractions of contact areas with ohmic characteristics were determined to be 2.1×10^{-8} and 1.5×10^{-8} for *control* and *cold-control* junctions, respectively. Table II shows the fraction of the ohmic regions, obtained as described here, for all five types of samples. While these ohmic fractions are miniscule, the current levels calcu-

TABLE II. Fractional amounts of the different types of contact for all samples. "Ohmic" contact refers to contact regions with very low barrier heights; the numerical values given below are calculated from the measured *RA*s and a nominal ohmic specific contact resistance ($10^{-6}\ \Omega\ \mathrm{cm}^2$) (see Sec. IV A). Au–GaAs "Schottky" contact refers to contact regions with barrier heights ~0.7 V or higher.

Samples	Au–GaAs ohmic	Au–GaAs Schottky	Au–dithiol–GaAs
control	2.1×10^{-8}	~1	0
cold-control	1.5×10^{-8}	~1	0
evaporated	5.5×10^{-9}	~0.35	~0.65
cold-evaporated	1.5×10^{-9}	~0.01	~0.99
nTP	7×10^{-14}	0	1

lated from Eq. (1) using these area fractions and $\Phi_{IV}=0$ V are consistent with the experimentally measured current levels. Hence, evaporating Au directly n^+ GaAs creates highly inhomogeneous Schottky contacts containing small regions of ohmic contact. Cooling the sample (*cold-control*) reduces the fraction of ohmic contact slightly, possibly due to the reduction of Au–GaAs reactivity at low temperatures. These ohmic regions strongly modify the Au–GaAs Schottky behavior in the $I-V$ characteristics of the *control* and *cold-control* samples despite the small fractions.

B. nTP junctions

For the Au–dithiol–GaAs devices made by nTP, the estimated ohmic fraction in the nTP junctions is $\sim7\times10^{-14}$ (Table II). This corresponds to an ohmic contact area of $\sim0.01\ \mathrm{nm}^2$ for the largest dots (area$=2\times10^{-3}\ \mathrm{cm}^2$). Since such a value is smaller than an atomic cross section, we thus conclude that areas of Au–n^+ GaAs ohmic contact are not present in the *nTP* junctions. Furthermore, the fact that Φ_{IV} for the *nTP* junctions (0.87 V) is higher than that expected for a Au–n^+ GaAs Schottky contact (0.7 V) signifies a different transport mechanism occurring in these junctions. Tunneling through an insulating barrier presented by the dithiol layer is consistent with lower J and higher Φ_{IV}.[38] Interestingly, junctions on the *nTP* sample have more ideal Schottky $I-V$ characteristics, i.e., lower n value, than the *control* and *evaporated* samples. This can be seen in Fig. 1(b): when the reverse J values are normalized, the forward J values for the *nTP* sample are higher than those for the *control* and *evaporated* samples. IPE results further support the notion of transport occurring through the molecular layer rather than through direct Au–GaAs contacts. If the transport mechanism were the same in all samples, we would expect the Y versus E curves to have the same shape for all samples with the magnitudes scaled according to the effective area. This is clearly not the case for the *nTP* junction (Fig. 2). Instead of a $(E-\Phi_{\mathrm{IPE}})^2$ dependence, the photoresponse in the nTP junctions follows $Y\propto\exp(E/E_0)$ for 3 1/2 decades. Thus, there is no direct Au–GaAs contact in the *nTP* junctions and electrical transport occurs through the molecular layer.

Note that while the small values of J in the *nTP* sample (Fig. 1) could be explained by a reduction of the effective contact area, the IPE results completely rule out this possibility. In addition to having a different E dependence but similar magnitude in the photoresponse yield for excitation below GaAs band gap, the above-band gap photoresponse yield in the *nTP* junctions is only a factor of 2 smaller than other samples [Fig. 2(a)]. For photon energies above the GaAs band gap, absorption occurs predominantly in the GaAs depletion region, producing electron–hole pairs that can separate and migrate to the electrodes (holes to Au and electron to n^+ GaAs, respectively). Since the photogenerated electrons can move readily into the GaAs bulk, transport of photogenerated holes to Au is the limiting step in the above-band gap photocurrent process. In the *nTP* junctions, the holes must traverse the dithiol molecular layer to reach the Au electrode since direct Au–GaAs contacts are absent. Hence, a good electrical path must exist between the Au and the GaAs. The reduced current density observed in $J-V$ curves for the *nTP* junctions must therefore be due to a different transport mechanism, rather than a smaller effective contact area.

The IPE yield is the convolution of the electron distribution in the emitter and the emission probability.[25] Hence, the energy dependence of IPE yield reflects the electron distribution in the emitter. For example, the usual $(E-\Phi_{\mathrm{IPE}})^2$ seen in metal–semiconductor Schottky contacts arises from the Fermi statistics of the electron density of states (DOS) in metals. An exponential E dependence, $Y\propto\exp(E/E_0)$, indicates that the emitter DOS has an exponential tail, with E_0 being the characteristic energy. In the *nTP* Au-1,8 octanedithiol–GaAs diodes, we obtained $E_0\sim50$ meV, which is substantially larger than kT and suggests the existence of disordered material.[39] Since the 1,8-octanedithiol molecules are relatively short, we expect the monolayer to contain significant disorder and defects. Scanning tunneling microscope images of alkanedithiol monolayer on Pt(111) reveal a highly defected layer with small ordered regions.[40] The high wave number measured for the CH_2 stretching mode is another indication of disorder. For alkanethiols, values above $2924\ \mathrm{cm}^{-1}$ indicate a liquid state of the monolayer.[41] While there is no comprehensive study on alkanedithiols, our result of $2927\ \mathrm{cm}^{-1}$ for the CH_2 stretching mode is consistent with a disordered dithiol monolayer. Therefore the disordered dithiol layer is the source of electrons for the below-band gap photoresponse in the nTP Au–dithiol–GaAs molecular diodes. Detailed studies will be published elsewhere.[31]

C. Evaporated junctions

Now that we have an understanding of the transport characteristics in Au–GaAs *control* and *nTP* Au–dithiol–GaAs junctions, let us examine the electrical behavior of Au–dithiol–GaAs diodes with evaporated Au electrodes (*evaporated* and *cold-evaporated*). The J values of these evaporated junctions are 1–2 orders of magnitude lower than those of the control junctions, but 4–5 orders higher than those of the *nTP* junctions. These evaporated junctions have similarly low Φ_{IV} and reverse-bias *RA* values as the control junctions,

indicating that Au–GaAs ohmic contacts also dominate the $I-V$ characteristics in molecular diodes with evaporated top contacts, despite the presence of the dithiol monolayer. The presence of Au–GaAs ohmic regions is further supported by the observation that $\Phi_{\mathrm{IPE}}>\Phi_{IV}$. The area fractions of ohmic contact for the *evaporated* and *cold-evaporated* samples are evaluated from their *RA*s and given in Table I.

For the *evaporated* sample, in which the Au evaporation was done without cooling the sample, the IPE result shows a classic $(E-\Phi_{\mathrm{IPE}})^2$ Schottky contact behavior with $\Phi_{\mathrm{IPE}}=0.7$ V [Fig. 2(b)], which is the same as Φ_{IPE} measured in the control junctions (*control* and *cold-control*) and consistent with the Au–GaAs barrier height. Hence, direct Au–GaAs Schottky contacts are present in the evaporated junctions. The ratio of the coefficient in front of $(E-\Phi_{\mathrm{IPE}})^2$ for the *evaporated* sample to the *control* sample provides a measure of the fraction of Au–GaAs Schottky contact in the *evaporated* sample, ~35% (Table II). This direct contact could arise from Au being deposited in the preexisting defects in the dithiol monolayer and/or additional damages that occur during the evaporation.

For the *cold-evaporated* sample, in which the sample temperature was maintained at −15 °C during Au evaporation, its IPE spectrum shows a clear $(E-\Phi_{\mathrm{IPE}})^2$ for $E<0.92$ eV even though it follows an exponential dependence similar to the nTP junctions for $E>1$ eV [Fig. 2(c)]. The solid line in Fig. 2(c) is a fit to the data using the combination of an exponential and 1% of the quadratic IPE yield of the *cold-control* sample. The IPE yield of the *cold-control* sample, which was made side by side with the *cold-evaporated* sample but contains no molecules, represents the IPE yield of a Au–GaAs Schottky contact with Au electrodes deposited at −15 °C. Hence, 1% of the junction areas in the *cold-evaporated* sample are Au–GaAs Schottky contact (Table II). Despite such a small percentage of direct Au–GaAs contact, the current densities of the *cold-evaporated* sample are 4 orders of magnitude higher than those of the *nTP* sample. This is attributed to the high reactivity between Au and GaAs, so that the existence of any direct contact will result in ohmic regions. Since the conductivity of these ohmic contacts is many orders of magnitude higher than transport through the molecular layer, a minute fraction of Au–GaAs ohmic contact will completely dominate the electrical transport in the molecular junctions. Thus, we infer that direct contacts between the two electrodes are unavoidable when the top Au electrodes are deposited by evaporation on the 1,8-octanedithiol layer.

D. Effect of sample temperature during metal evaporation

It is curious that cooling the samples to −15 °C during Au evaporation reduces the direct Au–GaAs contact fraction from 35% to 1%. A few possibilities come to mind: (1) damage to the molecular layer due to impinging high energy Au atoms; (2) condensation of contamination due to cooling the sample; (3) motion of Au atoms (e.g., diffusion and penetration) on and into the molecular layer; and (4) desorption or disordering of the molecular layer due to radiative heating. While the molecular layer can be damaged if the incoming Au atoms impart an amount of energy larger than a threshold (depending on bond strength), the Au atoms have kinetic energies approximately equal to the thermal energy at the melting point of Au (1062 °C) independent of the sample temperature. This energy is much larger than the thermal energy difference between the cooled and the uncooled sample (~50 °C). Hence, we do not expect reason (1) to be the dominant cause for the difference observed between the *evaporated* and *cold-evaporated* samples. Condensation of foreign substances on the cooling sample surface in high vacuum ($\leqslant 10^{-6}$ Torr) might "plug up" the defects in the monolayer, preventing the formation of direct Au–GaAs contacts in cooled samples. However, the cooled Au–GaAs (*cold-control*) sample, which was fabricated side by side with the *cold-evaporated* sample, has similar Φ_{IV}, Φ_{IPE}, and Φ_{CV} values to the uncooled Au–GaAs (*control*) sample. If condensation-induced contamination [factor (2)] were a big problem, one might expect the *control* and *cold-control* to exhibit more differences. Thus, the electrical characteristics of direct Au–GaAs contact are probably not significantly affected in the *cold-evaporated* sample. Currently we do not have enough data to differentiate between factors (3) and (4). As XPS results showed, the penetration of evaporated metal into the molecular layers depends on the molecule, the metal, their interaction, and the temperature, and is substantially minimized at low temperatures.[5] Hence, the difference we observed between the *evaporated* and *cold-evaporated* samples could be due to the temperature dependence of metal adatom mobility. However, we cannot rule out that the dithiol monolayer in the uncooled sample (*evaporated*) might develop more defects under radiative heating.

V. SUMMARY

In summary, the nature of electrical contacts in the Au–dithiol–GaAs system was studied by varying the fabrication method of the Au top electrodes. We found that direct Au–GaAs contacts always form when evaporating Au onto the dithiol molecular layer. Cooling the sample during evaporation helps to minimize direct contacts through the dithiol monolayer but does not eliminate their existence. In contrast, our results show that Au–dithiol–GaAs junctions made by the nTP method contain no direct contacts (electrical shorts) between the two electrodes. Hence, nTP is a very promising approach for fabricating molecular electronics. Furthermore, the $I-V$ and IPE results show that the 1,8-octanedithiol monolayer acts as an insulating tunnel barrier between Au and GaAs, with a broad distribution of DOS as inferred from IPE spectra, which is indicative of disorder in the molecular layer or inhomogeneity in bonding.

ACKNOWLEDGMENTS

The authors would like to thank K. West for the GaAs wafers, Y. Chabel for access to the FTIR, and A. Vilan, R. Tung, D. Monroe, D. Hammon, V. Bermudez, C. Varma, B. de Boer, and M. Lee for useful discussions.

[1]J. Reichert, R. Ochs, D. Beckmann, H. B. Weber, M. Mayor, and H. v. Lohneysen, Phys. Rev. Lett. **88**, 176804 (2002).
[2]J. M. Beebe, V. B. Engelkes, L. L. Miller, and C. D. Frisbie, J. Am. Chem. Soc. **124**, 11268 (2002).
[3]A. Vilan and D. Cahen, Adv. Funct. Mater. **12**, 795 (2002).
[4]J-O Lee, G. Lientschnig, F. Wiertz, M. Struijk, R. A. J. Janssen, R. Egberink, D. N. Reinhoudt, P. Hadley, and C. Deeker, Nano Lett. (2003).
[5]G. C. Herdt and A. W. Czanderna, J. Vac. Sci. Technol. A **12**, 2410 (1994); G. L. Fisher *et al.*, J. Am. Chem. Soc. **124**, 5528 (2002).
[6]R. E. Holmlin, R. Haag, M. L. Chabinyc, R. F. Ismagilov, A. E. Cohen, A. Terfort, M. A. Rampi, and G. M. Whitesides, J. Am. Chem. Soc. **123**, 5075 (2001).
[7]Y.-L. Loo, R. L. Willett, K. B. Baldwin, and J. A. Rogers, J. Am. Chem. Soc. **124**, 7654 (2002); Appl. Phys. Lett. **80**, 562 (2002).
[8]Y.-L. Loo, D. V. Lang, J. A. Rogers,and J. W. P. Hsu, Nano Lett. (to be published).
[9]C. W. Sheen, J.-X. Shi, J. Martensson, A. N. Parikh, and D. L. Allara, J. Am. Chem. Soc. **114**, 1514 (1992).
[10]T. Baum, S. Ye, and K. Uosaki, Langmuir **15**, 8577 (1999).
[11]D. B. Janes *et al.*, J. Vac. Sci. Technol. B **17**, 1773 (1999).
[12]S. M. Sze, *Physics of Semiconductor Devices*, 2nd ed. (Wiley, New York, 1981), p. 291.
[13]G. Myburg, F. D. Auret, W. E. Meyer, C. W. Louw, and M. J. van Staden, Thin Solid Films **325**, 181 (1998).
[14]In Ref. 11, p. 296.
[15]Y.-L. Loo, J. W. P. Hsu, R. L. Willett, K. B. Baldwin, K. W. West, and J. A. Rogers, J. Vac. Sci. Technol. B **20**, 2853 (2002).
[16]Gold nanoparticles are unfunctionalized; used as received from Ted Pella Inc.
[17]This measured density is limited by the AFM resolution.
[18]C. Kim, P. E. Burrows, and S. R. Forrest, Science **288**, 831 (2000).
[19]This is one of eight nTP samples we measured. The *RA* values of the 88 diodes measured on all nTP samples are within an order of magnitude: $(1.65\pm1.07)\times10^7\ \Omega\ \mathrm{cm}^2$.
[20]E. H. Rhoderick, *Metal-Semiconductor Contacts*, 1st ed. (Oxford University Press, Oxford, 1978), p. 87.
[21]In Ref. 11, p. 257.
[22]A. Vilan, A. Shanzer, and D. Cahen, Nature (London) **404**, 166 (2000); A. Vilan, PhD thesis, Weizmann Institute of Science, 2001.
[23]T. Ishida and H. Ikoma, J. Appl. Phys. **74**, 3977 (1993).
[24]In Ref. 11, Chap. 5.5.2.
[25]R. J. Powell, J. Appl. Phys. **41**, 2424 (1970).
[26]In Ref. 11, p. 286.
[27]F. A. Padovani and G. G. Summer, J. Appl. Phys. **36**, 3744 (1965); Yu. A. Gol'dberg, E. A. Posse, and B. V. Tsarenkov, Sov. Phys. Semicond. **9**, 337 (1975).
[28]L. C. Chen, D. A. Caldwell, T. G. Finstad, and C. J. Palmstrom, J. Vac. Sci. Technol. A **17**, 1307 (1999).
[29]In Ref. 11, p. 391.
[30]H. Ishii, K. Sugiyama, E. Ito, and K. Seki, Adv. Mater. **11**, 605 (1999); N. J. Watkins, L. Yan, and Y. Gao, Appl. Phys. Lett. **80**, 4384 (2002); S. Crispin, V. Geskin, A. Crispin, J. Cornil, R. Lazzaroni, W. R. Salaneck, and J.-L. Bredas, J. Am. Chem. Soc. **124**, 8131 (2002).
[31]J. W. P. Hsu, D. V. Lang, Y. L. Loo, and K. Raghavachari, preprint.
[32]In Ref. 19, Chap. 3.3.1.
[33]R. T. Tung, Mater. Sci. Eng., R. **35**, 1 (2001); R. T. Tung, Phys. Rev. B **45**, 13509 (1992).
[34]J. H. Werner and H. H. Guttler, J. Appl. Phys. **69**, 1522 (1991).
[35]W. J. Kaiser, L. D. Bell, M. H. Hecht, and F. J. Grunthaner, J. Vac. Sci. Technol. B **7**, 945 (1989).
[36]V. G. Weizer and N. S. Fatemi, J. Appl. Phys. **64**, 4618 (1988).
[37]D. V. Morgan and J. Wood, *Properties of Gallium Arsenide*, 2nd ed. (INSPEC, New York, 1990), Chap. 16.1.
[38]C. Boulas, J. V. Davidovits, F. Rondelez, and D. Vuillaume, Phys. Rev. Lett. **76**, 4797 (1996).
[39]G. A. N. Connell, in *Amorphous Semiconductors*, edited by M. H. Brodsky (Springer, New York, 1979), Chap. 4.
[40]J.-S. Yang, C.-C. Lee, S.-L. Yau, C.-C. Chang, C.-C. Lee, and J.-M. Leu, J. Org. Chem. **65**, 871 (2000).
[41]M. D. Porter, T. B. Bright, D. L. Allara, and C. E. D. Chidsey, J. Am. Chem. Soc. **109**, 3559 (1987).